

Multiple Fireball Formation And Rapidity Spectra Of Proton-Antiproton Flow At $\sqrt{s_{NN}} = 200$ GeV RHIC Energy

Jan Shabir Ahmad

Department of Physics, Govt. Sri Pratap College,
Srinagar, J&K

Abstract: We invoke the multiple fireball formation model proposed recently to understand the $p - \bar{p}$ data and \bar{p}/p data. The model is used to describe the rapidity spectra of protons and antiprotons measured at the highest energy of Relativistic Heavy Ion Collider, $\sqrt{s_{NN}} = 200$ GeV by BRAHMS Collaboration. We have also determined the contribution of the decay products of the heavier resonances like Δ , Λ etc. to the rapidity spectra of the protons and antiprotons. We find that their contributions actually dominate over the protons (antiprotons) of pure thermal origin. We have also imposed the criteria of exact strangeness conservation in each fireball separately. It is shown that it is possible to explain the complete set of data viz. the rapidity distribution of protons, antiprotons, net protons ($p - \bar{p}$) and the ratio \bar{p}/p simultaneously quite well with a single set of model parameters and a single value of the temperature parameter T chosen for all the fireballs. This is unlike the previous analyses wherein a varying temperature has been assumed for the fireballs formed along the rapidity axis. The chemical potentials are however assumed to be dependent on the fireball rapidity y_{FB} .

PACS Numbers: 24.10.Pa, 24.10.-I, 25.75-q, 25.75 Dw

Keywords: thermal model, ultrarelativistic nuclear collision, rapidity distribution

I. INTRODUCTION

The yields of baryons and antibaryons are an important indicator of the multi-particle production phenomenon in the ultra-relativistic nucleus-nucleus collisions. Great amount of experimental data have been obtained in such experiments ranging from the AGS energies to the RHIC. The study of ultra-relativistic nuclear collisions allows us to learn how baryon numbers, initially carried by the nucleons, are distributed in the final state [1]. It is possible to obtain important information about the energy loss of the colliding nuclei by analyzing the rapidity dependence of the p and \bar{p} production. The measurement of the net proton flow (i.e. $p - \bar{p}$) in such experiments can throw light on the collision scenario, viz. the extent of nuclear stopping, formation of the

fireball and the degree of thermo-chemical equilibration of heavier resonances (Δ etc.) which can be estimated by their contribution to lighter hadrons, say, p and \bar{p} via their decay. The net proton flow at the AGS energies peaks at midrapidity, while at the top SPS energy ($\sqrt{s_{NN}} = 17$ GeV) the distribution develops a minimum at midrapidity. The SPS data at different energies (20, 30, 40, 80, 158 GeV/A) show [1] that at midrapidity the p yield decreases gradually with increasing energy in contrast to the rapidly rising \bar{p} yield. This implies that at SPS energies nuclear collisions start exhibiting some transparency. Recently a new property has emerged namely the extended longitudinal scaling in the rapidity distributions [2 - 5]. This has been observed in pp collisions as well as ultra-relativistic collisions at the highest RHIC energies [5, 6].

Data from the BRAHMS collaboration [7] show that the antiproton to proton ratio shows a maximum at mid rapidity and gradually decreases towards larger rapidities, whereas the net proton flow shows a broad minimum, spanning about ± 1 unit around mid-rapidity region of dN/dy spectra. It was therefore conjectured [7] that at RHIC energies the collisions are quite transparent. The midrapidity region at RHIC is not yet totally baryon free however a transition from a baryon dominated system at lower energies to an *almost* baryon free system in the midrapidity at RHIC can be observed. An interesting analysis by Stiles and Murray [2,8] shows that the data obtained by the BRAHMS collaboration at 200 GeV has a clear dependence of the baryon chemical potential on rapidity due to the changing \bar{p}/p ratio. Biedron and Broniowski [2,9] have done an analysis of rapidity dependence of the \bar{p}/p , K^+/K^- , π^+/π^- ratios based on a single freeze-out model of relativistic nuclear collisions. Fu-Hu Liu *et al.* have [10] have recently attempted to describe the transverse momentum spectrum and rapidity distribution of net protons produced in high energy nuclear collisions by using a new approach viz. a two cylinder model [11 - 13]. In order to describe the rapidity distribution of the produced hadrons in ultrarelativistic nuclear collisions the statistical thermal model has been extended to allow for the chemical potential and temperature to become *rapidity dependent* [5, 9, 14 - 16]. Recently Becattini *et al.* and Cleymans *et al.* [2, 5, 14 - 16] have attempted to describe the net proton flow data obtained at RHIC in Au - Au collisions at 200 GeV. They have applied the thermal model in a very interesting way where they consider the rapidity axis to be populated with fireballs moving along it with increasing rapidity, y_{FB} . The emitted particles leave the fireballs at freeze-out following a thermal distribution. The rapidity distribution of any given particle specie j can then be written as:

$$\frac{dN^j(y)}{dy} = \int_{-\infty}^{+\infty} \rho(y_{FB}) \frac{dN_1^j(y - y_{FB})}{dy} dy_{FB} \quad (1)$$

where y is the particle's rapidity. The distribution $\frac{dN^j(y)}{dy}$

represents total contribution of all the fireballs to the j^{th} hadron specie's rapidity spectra. This also includes the contribution of the decay products of heavy resonances. The contribution of the respective fireballs follows a Gaussian distribution centred at zero fireball rapidity ($y_{FB} = 0$):

$$\rho(y_{FB}) = \frac{1}{\sqrt{2\pi}\sigma} \exp\left(\frac{-y_{FB}^2}{2\sigma^2}\right) \quad (2)$$

The value of σ determines the width of the distribution. The data essentially require a superposition of fireball contributions along the rapidity axis where the baryon chemical potential (μ_B) of the successive fireballs is depended on the fireball rapidity (y_{FB}). A quadratic type dependence is considered [2, 4]:

$$\mu_B = a + b y_{FB}^2 \quad (3)$$

In the recent works [5, 17] it has been further assumed that the temperature of the successive fireballs along the

rapidity axis *decreases* (as the baryon chemical potential increases) according to a chosen parameterization:

$$T = 0.166 - 0.139 \mu_B^2 - 0.053 \mu_B^4 \quad (4)$$

where the units are in GeV. Here the temperature of the mid-rapidity fireball ($y_{FB} \sim 0$) is fixed at 166 MeV.

In the work of Becattini and Cleymans [2, 4] a good fit to the net proton flow as measured at the highest RHIC energy by the BRAHMS collaboration has been obtained. The values of the model parameters fitted by them at the highest RHIC energy are, $a = 23.8$ MeV, $b = 11.2$ MeV and $\sigma = 2.183$. The temperature T varies according to the parameterization (4).

However, there is no fit provided for the \bar{p}/p data or the proton and antiproton data independently.

In this letter we have attempted to use the above discussed multi-fireball model to explain the proton flow, anti proton flow, net proton flow (i.e. $p - \bar{p}$) and the ratio

\bar{p}/p simultaneously with a single set of model parameters (viz. a, b, σ) which also includes a single value of the temperature parameter T chosen for all the fireballs. This is unlike the previous analyses wherein a varying temperature has been assumed for the fireballs formed along the rapidity axis. The chemical potentials are however still assumed to be dependent on the fireball rapidity y_{FB} , a situation which is unavoidable in the model, due to the nature of the data.

In figures 1 and 2 we have shown the experimental dN/dy data (by the red solid boxes) for the protons and antiprotons, respectively, obtained from the top 5% most central collisions at $\sqrt{s_{NN}} = 200$ GeV in the BRAHMS experiment. The errors are both statistical and systematic. The proton and antiproton dN/dy decrease from midrapidity to $y \sim 3$. We have fitted both spectral shapes simultaneously for $a = 18.5$, $b = 12.2$, $\sigma = 1.89$ and $T = 172.5$ MeV. We find that the theoretical curves fit the data quite well in both the cases. The experimental data have been symmetrized for the negative values of rapidity [7]. The weighted χ^2/DoF for the two fits in figures 1 and 2 are 0.33 and 0.36, respectively.

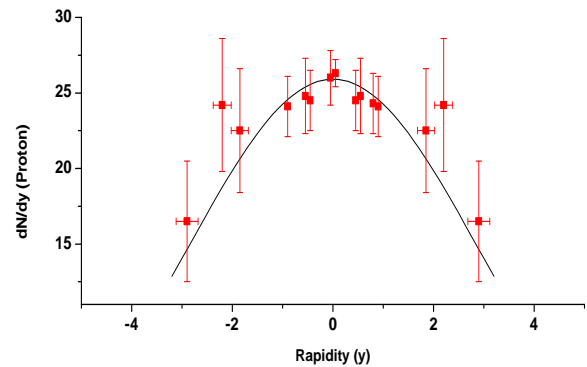


Figure 1: Proton rapidity spectra. The square solid boxes are the BRAHMS experimental data points. The theoretically calculated values are shown by the solid curve

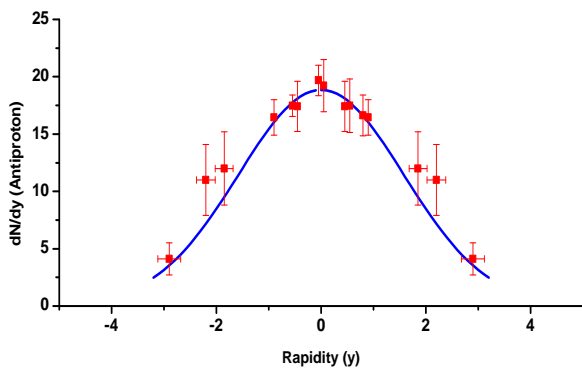


Figure 2: Antiproton rapidity spectra. The square solid boxes are the BRAHMS experimental data points. The theoretically calculated values are shown by the solid curve

Figure 3 shows the rapidity spectra dN/dy for the net proton flow. The theoretical curve which fits the data for the same values of the model parameter mentioned above is also shown. There is somewhat a broad minimum around the midrapidity region. The situation is not as was expected widely [18] that the rapidity distribution of hadrons produced in the relativistic nuclear collisions will exhibit a plateau, centred at midrapidity. So far it has not been observed, either in the SPS experiments or at the RHIC. Moreover the proton spectra in the figure 1 is seen to be slightly broader than the antiproton spectra in figure 2. This seems to emerge from the fact that since the rapidity axis is assumed to be populated by the fireballs of successively increasing rapidity y_{FB} and hence increasing chemical potential, the low rapidity (y) hadrons (which have a larger population in a baryon rich fireball in thermo-chemical equilibrium) emitted in the forward (backward) direction from a fast fireball (i.e. fireballs with large y_{FB}), appear with a large value of rapidity (y) in the rest frame of the colliding nuclei. In other words as the baryon chemical potentials (μ_B) increase monotonically along the rapidity axis (as $\sim y_{FB}^2$) there is an increase in the density of the protons (and a suppression in the density of antiprotons) as we move away from the mid rapidity region to $y \sim 2.2$. The χ^2/DoF for the fitted curve is 0.69.

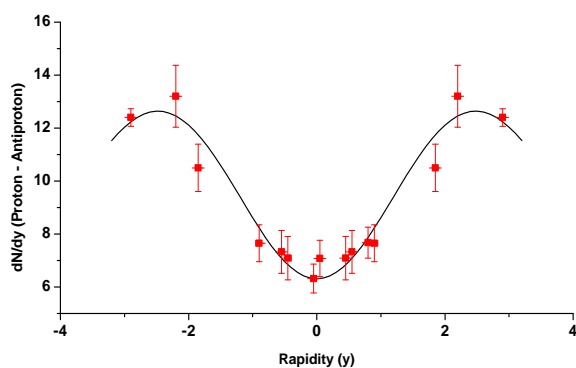


Figure 3: Rapidity spectra of the net proton flow. The theoretical curve which fits the data is for the same values of

the model parameters as used for the theoretical curves in figures 1 and 2

In figure 4 we have shown the rapidity spectra of the \bar{p}/p ratio. The ratio has somewhat a broad maximum (~ 0.75) in the midrapidity region which then decreases to about 25% at around $y \sim 3$. The theoretical curve shown is again for the same values of the parameters as mentioned above. We find that the curve provides a reasonably good fit to the experimental data. The χ^2/DoF is 1.9 in this case. This relatively larger value seems to emerge due the relatively smaller error bars involved here with the \bar{p}/p data as compared to the p and \bar{p} data sets.

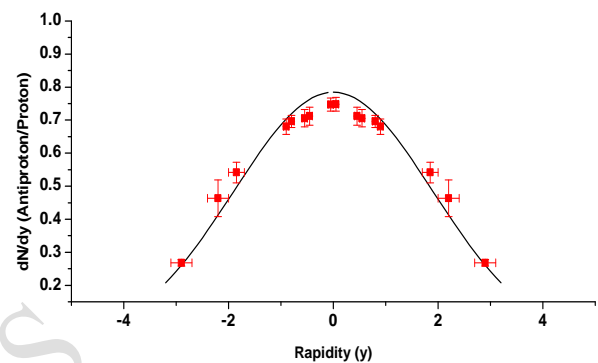


Figure 4: Rapidity spectra of antiproton/proton ratio. The calculated rapidity distribution is shown by the curve

In the analysis we have also included the contribution of the decay protons and antiprotons (from the Δ , Λ etc.). It is interesting to find that the contributions of the decaying hadronic resonances actually dominate over the protons and antiprotons of pure thermal origin (i.e. those which are not the decay products). This effect is highlighted in figure 5 for the net proton flow. The lowest (green dashed) curve is the contribution of the pure thermal protons (antiprotons) to the net proton flow while the next upper (magenta dashed-dotted) curve shows the contribution of the heavier particles decaying to protons (antiprotons). The solid (black) curve is again the total value (as shown in figure 3 also). It is worthwhile to note that the shape of the theoretical spectra is almost same for both the cases i.e. for the pure thermal and the decay products. To understand this better we have shown in figure 6 a rescaled curve of the pure thermal net protons where we have multiplied the theoretical data points by a factor of 5. We see that the shapes of all these curves are almost identical. Hence we find that the contribution of the decaying particles does not alter the shape of the final net proton spectra to any significant extent in the present model. Similarly in the figures 7 and 8 we have shown the contributions of the decay products (magenta dashed-dotted curves) to the proton and antiproton spectra, respectively. The pure thermal contributions (green dashed curves) are again rescaled to enable a comparison of their shapes with the shape of decay products and total spectra. It is again seen that all the three curves have almost identical shapes.

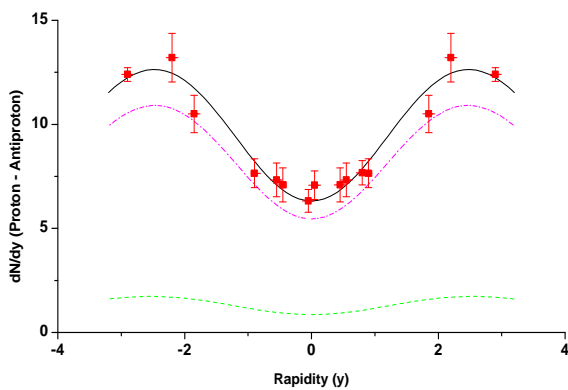


Figure 5: Rapidity spectra of the net proton flow for the same values of the model parameters as used for the theoretical curves in figures 1 and 2. The lowest (green dashed) curve is the contribution of the pure thermal protons (antiprotons) to the net proton flow while the next upper (magenta dashed-dotted) curve shows the contribution of the heavier particles decaying to protons (antiprotons). The solid (black) curve is again the total value (as shown in figure 3 also)

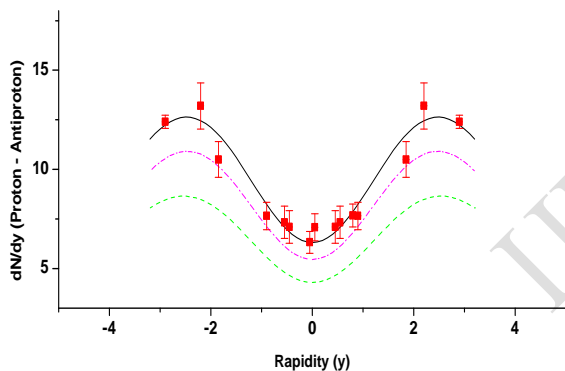


Figure 6: Same as figure 5 but with the contribution of the pure thermal protons (antiprotons) scaled up (green dashed curve) by factor 5 to enable a comparison of the shape of the three spectra

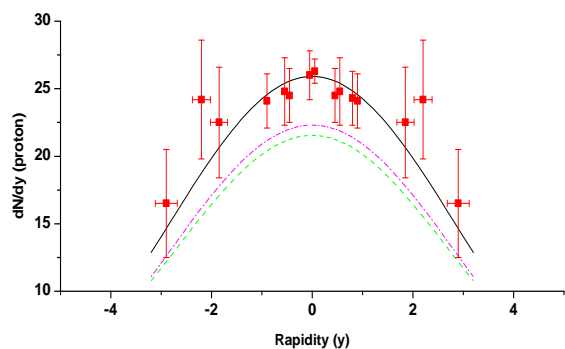


Figure 7: Rapidity spectra of the proton flow. The theoretical curves are for the same values of the model parameters as used in figures 1 - 4. The lowest (green dashed) curve is the

contribution of the pure thermal protons (which is rescaled to enable a comparison of the shape of the three spectra. The next upper (magenta dashed-dotted) curve shows the contribution of the heavier particles decaying to protons). The solid (black) curve is the total value as in figure 1

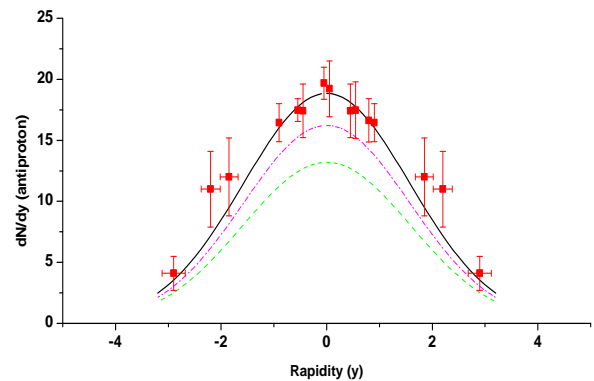


Figure 8: Rapidity spectra of the antiproton flow. The theoretical curves are for the same values of the model parameters as used in figures 1 - 4. The lowest (green dashed) curve is the contribution of the pure thermal antiprotons (which is rescaled to enable a comparison of the shape of the three spectra. The next upper (magenta dashed-dotted) curve shows the contribution of the heavier particles decaying to protons). The solid (black) curve is the total value as in figure 2

In our analysis we have applied the criteria of exact strangeness conservation. It is done in a way such that the net strangeness is zero not only on the overall basis but also in every fireball separately. This is essential because as the rapidity of the fireballs formed increases along the rapidity axis the baryon chemical potential (μ_B) increases. Hence the required value of the strange chemical potential (μ_S) varies accordingly for each fireball for a given value of temperature $T (= 172.5 \text{ MeV}$ here). Consequently the values of the strange chemical potential (μ_S) will vary with y_{FB} . In figure 9 we have shown this by plotting the variation of the μ_S with y_{FB} . It is seen to first rise smoothly with y_{FB} reaching a maximum value of about 50 MeV at around $y_{FB} \sim 3.5$ and then drops rapidly to very small values as $y_{FB} \sim 5$.

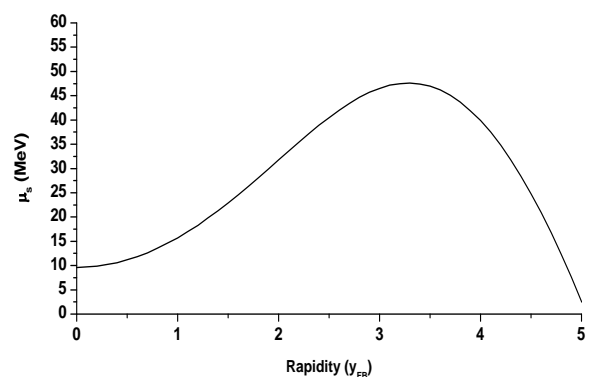


Figure 9: The variation of the μ_S with y_{FB} for $T = 172.5 \text{ MeV}$

In summary, we use the thermal model where formation of several fireballs moving with increasing rapidity (y_{FB}) along the rapidity axis is assumed. A Gaussian profile in y_{FB} is used to provide a weight factor to estimate their contribution to the emitted hadrons population. A quadratic profile in y_{FB} is used to fix the baryon chemical potentials of these fireballs. We find that it is possible to explain not only the proton and antiproton rapidity spectra separately but also the net proton flow and the \bar{p}/p ratio simultaneously. This is done by using a *single* set of the model parameters. This is unlike the previous analyses of the RHIC data where a theoretical fit to the proton, antiproton and the \bar{p}/p ratio spectra was not shown and the temperature T of the individual fireballs was assumed to vary continuously with y_{FB} .

REFERENCES

- [1] E. Kornas *et al.* NA 49 Collaboration, Eur. Phys. J. C49 (2007) 293.
 [2] F. Becattini *et al.* arXiv: 0709.2599v1 [hep-ph].
 [3] Fu-Hu Liu *et al.*, Europhysics Letters 81 (2008) 22001.
 [4] J. Cleymans, J. Phys G35 (2008) 1.
 [5] J. Cleymans *et al.* arXiv: 0712.2463v4 [hep-ph] 2008.
 [6] G. J. Alner *et al.* Z. Phys. C33 91986) 1.
 [7] I. G. Bearden *et al.*, BRAHMS Collaboration, Phys. Rev. Lett. 93 (2004) 102301.
 [8] L. A. Stiles and M. Murray, nucl-ex/0601039.
 [9] B. Biedroń and W. Broniowski, Phys. Rev C75 (2007) 054905.
 [10] Fu-Hu Liu *et al.*, Europhys. Lett. 81 (2008) 22001.
 [11] Fu-Hu Liu *et al.*, Phys. Rev C69 (2004) 034905.
 [12] Fu-Hu Liu, Phys. Rev. C66 (2002) 047902.
 [13] Fu-Hu Liu, Phys. Lett. B583 (2004) 68.
 [14] F. Becattini and J. Cleymans, J. Phys. G34 (2007) S959.
 [15] F. Becattini *et al.*, Proceedings of Science, CPOD07 (2007) 012,
 [16] W. Broniowski and B. Biedroń J. Phys. G35 (2008) 044018, arXiv: 0709.0126 [nucl-th].
 [17] J. Cleymans *et al.* Phys. Rev. C75 (2006) 034905.
 [18] J. D. Bjorken, Phys. Rev. D27 (1983) 140.